The Peculiar Kinetics of the Reaction between Acetylene and the Cyclopentadienyl Radical

Simone Fascella, Carlo Cavallotti,* Renato Rota,* and Sergio Carrà

Politecnico di Milano, Dipartimento di Chimica, Materiali e Ingegneria Chimica "G. Natta" / CIIRCO, Via Mancinelli 7, 20131 Milano, Italy

Received: March 23, 2005; In Final Form: June 20, 2005

The cyclopentadienyl radical (cC_5H_5) is a fascinating molecule characterized by several peculiar properties, such as its high internal symmetry and resonance enhanced stability. This makes cC_5H_5 one of the most abundant radicals present in high temperature gaseous environments, such as flames. Therefore it is generally considered an interesting candidate as the starting point of reaction pathways leading to the formation of polycyclic aromatic hydrocarbons (PAH) and soot in combustion processes. However, known reaction pathways are not able to explain some recent experimental findings concerning the rapid conversion of cC_5H_5 into C_7H_7 and C_9H_8 in the presence of acetylene. In this work, we used ab initio calculations and quantum Rice−Ramsperger−Kassel (QRRK) theory to investigate the $cC_5H_5 + C_2H_2$ reaction kinetics. We found that cC_5H_5 can add acetylene to form, through a fast and not previously known reaction, the heptatrienyl radical (cC_7H_7), which, in many ways, can be considered the superior homologue of cC_5H_5. The calculated reaction kinetic constant is $(2.2 \times 10^{11})\exp(-6440/T(\mathrm{K}))$ cm^3 mol^{-1} s^{-1} and is in good agreement with experimental data, while that of the inverse process is $(4.2 \times 10^{16})T^{-1} \exp(-30\,850/T(\mathrm{K}))$ s^{-1}. In a successive reaction, cC_7H_7 can add a second acetylene molecule to form indene, cC_9H_8, and H. The forward and backward kinetic constants are $(6.6 \times 10^{11})\exp(-10\,080/T(\mathrm{K}))$ and $(4.2 \times 10^{14})\exp(-27\,300/T(\mathrm{K}))$ cm^3 mol^{-1} s^{-1}, respectively. These two successive reactions, leading from a single C5 cycle to a bicyclic C5−C6 species, represent a new PAH growth mechanism, characterized by a C5−C7 ring enlargement reaction.

1. Introduction

The cyclopentadienyl radical (in the following referred to as cC_5H_5) is a fascinating molecule characterized by many particular and almost unique properties. It has a high internal symmetry with a 5-fold degenerate rotational axis and a rotational symmetry number of 10. The structure is distorted from that of a regular pentagon by a large Jahn−Teller effect, which influences its vibrational and rotational entropy[1]. Moreover, this radical is highly stabilized by five resonant structures, and the corresponding $cC_5H_5^-$ anion is aromatic. Because of its thermodynamic stability, cC_5H_5 can be easily produced in the gas phase, either through laser photolysis or, more generally, during the combustion of hydrocarbons as one of the most abundant hydrocarbon radicals.[1−3] These unusual properties have motivated many theoretical and experimental studies on this molecule aimed to investigate various aspects of its structure and reactivity.[1,4−10] However, despite these recent investigations, the reactivity of cC_5H_5 is not yet fully understood. Qualitatively, there is a large agreement that the chemistry of cC_5H_5 plays a significant role in the formation of naphthalene and phenanthrene and, consequently, in the formation of polycyclic aromatic hydrocarbons (PAH_S) and soot.[11−15] This is very important since nowadays it is well accepted that air pollution is related to lung cancer and cardiopulmonary disease[16] and at least a part of the health hazard of atmospheric pollution can be related to PAHs, some of which have been found to be mutagenic,[17] and soot, which represents a major fraction of atmospheric aerosols. Consequently, much attention has to be paid to the emissions of PAHs and soot from fossil fuel combustion[18] since it will represent, at least for the next decades, the main source of power for humanity.

The minimization of the formation of PAHs and soot in combustion processes would allow for development of new and cleaner burners and engines, but it requires the control of the chemical processes responsible for their formation and growth. This will be possible only on the basis of a better physical and chemical understanding of such reaction pathways. Although, as previously mentioned, many important details on PAH and soot formation and growth are not yet completely understood, there is a general agreement that the process starts with the formation of molecular precursors of soot (that is, heavy PAHs of molecular weight 500−1000 amu) from smaller molecules, followed by their growth through addition of gaseous molecules or reactive particle−particle collisions. A slightly different view recently proposed involves the polymerization of small PAHs to form high molecular mass compounds,[19] instead of the growth of light PAHs by addition of small molecules and cyclization.

In any case, it is quite well established that small PAH formation precedes soot inception and proceeds through reaction paths involving lighter cyclic hydrocarbons, such as cC_5H_5. Therefore, kinetic information concerning the formation of small cyclic hydrocarbons plays an important role in defining the chemical reaction pathways responsible for PAH and soot formation. In this framework, the importance of fundamental studies aimed at elucidating at least the relative rates of different reaction channels leading to small PAHs is clear. This would allow researches to confirm or rule out some reaction patterns.

In this framework, a recent experimental work[20] clearly showed that cC_5H_5 can react with acetylene to form C_7H_7 and, successively, C_9H_8. This finding is very interesting, since

* To whom correspondence should be addressed. E-mail: carlo.cavallotti@polimi.it. Tel: ++39-02-23993176. Fax: ++39-02-23993180.

10.1021/jp051508x CCC: $30.25
Published on Web 07/28/2005

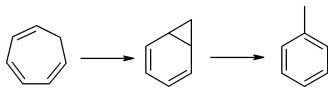

Figure 1. A possible pathway for the conversion of cycloheptatriene into toluene.

acetylene can be present in high concentration in flames, both at high and low temperatures, because of its great thermodynamic stability. Therefore, if it can react rapidly with cC_5H_5, which can be also present in high concentration in flames, to form larger molecules, these reactions can provide a new formation pathway of PAHs, which, if fast enough, might contribute significantly to the overall rate of formation of soot. This was not deeply investigated in the aforementioned experimental work since its main aim was to study the rate of formation of cC_5H_5 from the propargyl radical, C_3H_3, and C_2H_2. The experiments were performed using laser photolysis to generate C_3H_3 radicals, which, in the presence of C_2H_2, reacted to form cC_5H_5. The concentration of the relevant gas-phase species was measured with mass spectrometry. Though the focus of the work was to measure the rate of formation of cC_5H_5, it was found that, once produced, it can react successively with C_2H_2. However, the chemical identity of the products of the reaction, namely, C_7H_7 and C_9H_8, could not be established on the basis of the experimental data alone.

The experimental evidence that the addition of cC_5H_5 and C_2H_2 results in the formation of an undetermined C_7H_7 species opens up an extremely interesting field of investigation. It is in fact known that a very similar molecule, cycloheptatriene (cC_7H_8), can have a very rich chemistry, because it can exist in at least six different isomers that, at relatively low temperatures, can be interconverted among the isomers. In particular, bicyclo-[2.2.1]hepta-2,4-diene (norbornadiene) can thermally isomerize to form, in succession, a biradical species, bicyclo[4.1.0]hepta-2,4-diene (norcardiene), 1,3,5-cycloheptatriene, a corresponding diradical, and, eventually, toluene. The kinetics of the thermal C_7H_8 isomerization has been extensively investigated both experimentally[21] and theoretically.[22] It was found that the internal rearrangements are determined by ring opening and closing reactions and by hydrogen transposition reactions, which determine the interconversion of the C_7H_8 isomers, as shown in Figure 1.

It appears thus reasonable that, if a C_7H_7 reactive radical, sufficiently stable to survive to its decomposition into cC_5H_5 and C_2H_2, is formed in the gas phase, it can give rise to an analogous rich chemistry.

Consequently, the main aim of the present investigation was to study, from a theoretical point of view, the kinetics of the reaction between the cyclopentadienyl radical and acetylene. The theoretical approach that we adopted is based on the ab initio integration of the time-independent Schrödinger equation for the calculation of structures and energies of reactants, products, and transition states. Kinetic constants of elementary reactions are determined with classic transition state theory, which, as shown recently,[23] can provide very reasonable estimation of reaction rates provided that the potential energy surface is known with sufficient accuracy and that the temperature is sufficiently high to make quantum tunneling effects negligible. Kinetic constants of complex reactions, that is, reactions in which several competitive elementary processes are possible for the same excited complex, were calculated with quantum Rice−Ramsperger−Kassel (QRRK) theory.[24] We hypothesized several reaction mechanisms using as a basis for our guesses chemical intuition and a certain understanding of the kinetics of similar processes. To test whether our hypotheses were acceptable or needed to be reconsidered, we compared the calculated QRRK rates with experimental rates measured at 1000 K.[20] This approach, described in more detail in the next section, led us to reject several mechanisms, of which we discuss only the most significant in the Results and Discussion section of this paper, before finding the one that could explain the experimental data.

2. Method and Theoretical Background

The reactions here investigated are complex processes that involve several elementary steps. To correctly take into account the probability to form different excited intermediates and their mutual interconversion, we used QRRK theory as modified by Dean[24] for bimolecular reactions. The reference equations are the same as those that we described in our previous studies.[25−27] In particular, the kinetic constant of each reaction *i* involving the *k*th excited complex, C*, can be calculated from QRRK theory as

$$k_i^{\mathrm{rxn}} = \sum_{E=E_{\mathrm{crit}}}^{\infty} k_i(E)[\mathrm{C}^*]f(E) \qquad (1)$$

where E_{crit} is the activation energy for the considered reaction, measured from the bottom of the potential energy well for each excited species, and $f(E)$ is the corresponding chemical activation distribution function.

The parameters required by QRRK are the rate of intermolecular energy transfer between excited and nonexcited species, the kinetic constants (preexponential factor and activation energy) for each elementary reaction, and the mean vibrational frequencies for every chemical species involved in the global kinetic scheme. The kinetic parameters and mean vibrational frequencies were calculated using ab initio methods as discussed in the following. The intermolecular energy transfer was calculated using the energy transmission factor suggested by Troe[28] assuming that the mean energy transferred per collision is 980 cal/mol. All QRRK calculations were performed at 1 atm. For each elementary reaction, forward kinetic constants were evaluated with quantum chemistry and transition state theory, while backward kinetic constants were determined by applying thermodynamic consistence (i.e., from the equilibrium constant) with calculated enthalpy and entropy changes. All calculations were performed using the Gaussian 98 program suite[29] at different levels of theory. Geometries were optimized using density functional theory (DFT), with exchange and correlation energies calculated with the Becke three-parameter and Lee−Yang−Parr functionals (B3LYP)[30,31] using the 6-31G(d,p) basis set. Frequency calculations were performed at the same level of theory both to calculate the vibrational frequencies of each adduct, required as input to QRRK, and to verify the stability of reactants, products, and transition states. In particular, stable chemical species were characterized by the absence of imaginary frequencies, while calculated transition state (TS) structures were characterized by the presence of a single imaginary frequency.

When found to be necessary to improve the level of description of the system, the energy of every molecule was calculated using an approach similar to G2MP2, to which we refer in the following as G2MP2*.[32] The energy of the molecule is first calculated at the QCISD(T)/6-311+G(d,p) level on structures optimized at the B3LYP/6-31G(d,p) level and corrected for the basis set error, subtracting the energy calculated at the MP2/6-311+G(d,p) level from that calculated at the MP2/6-311+G(3df,2p) level. The procedure of the calculation is

described in detail in our previous work.[27] G2MP2* increases the accuracy of the calculated energies with respect to DFT at the expanse of a significant increase of the computational time. In summary, the molecular energy was calculated as

$$E = E(\text{QCISD(T)/6-311+G(d,p)}) + E(\text{MP2/6-311+G(3df,2p)}) - E(\text{MP2/6-311+G(d,p)}) + \text{ZPE} + \text{TE} + \text{HLC} \quad (2)$$

where HLC is the higher level correction term proposed for the original G2MP2 theory[32] and TE is the thermal contribution to energy at 300 K. Kinetic constants of elementary reactions were calculated using classic transition state theory[33] and corrected for tunneling with the Wigner approximation.[34]

Finally the possibility that low vibrational frequencies might degenerate in torsional rotors was analyzed for reactants, products, and transition states. Thus, as a general rule, we calculated the potential energy as a function of the rotation angle for internal motions corresponding to torsional vibrational frequencies smaller than 150 cm^{-1}, from which we determined the hindered rotor partition function.[27]

3. Results and Discussion

The systematic study of the reactions that can follow the addition of C_2H_2 to the cyclopentadienyl radical has led to the investigation of several different hypotheses of reaction pathways. The investigated mechanisms can be divided in three major classes: hydrogen abstraction carbon addition reactions (HACA); addition−stabilization without opening of the C_5 ring (AcAc); addition−stabilization with opening of the C_5 ring (C_7).

The kinetics of all the possible reactions were investigated with DFT at B3LYP/6-31G(d,p) level, as described in the previous paragraph. The level of accuracy of these calculations was in fact judged to be sufficient to identify which is the dominant reaction pathway. For the last mechanism only, which was found to be significantly faster than the other two, energies were evaluated at the G2MP2 level on structures optimized at the DFT level.

3.1. HACA Mechanism. The first $C_2H_2-C_5H_5$ reaction mechanism analyzed corresponds to the "HACA" mechanism proposed by Frenklach et al.[35] to describe the growth of PAH. In the HACA mechanism, the PAH growth from the first aromatic ring, that is, benzene, takes place through a succession of reactions. First, atomic hydrogen reacts with benzene to give the benzyl radical, which in turn reacts with C_2H_2 to give acetylbenzene and atomic hydrogen. The growth to naphthalene involves two successive similar reactions: the abstraction of a H atom by a H radical to create a radical species with the unpaired electron delocalized on the aromatic ring, followed by the reaction of this intermediate species with C_2H_2 to give the $C_{10}H_7$ species. The last reactions are the ring formation and the addition of a hydrogen radical leading to naphthalene. The mechanism that we have studied for the reaction between C_2H_2 and C_5H_5, schematically represented in Figure 2, follows the same lines.

The mechanism is initiated by the reaction of cC_5H_5 with C_2H_2 to give a linear adduct, $C_7H_7^l$, formed by a ring of five carbon atoms and an acetylene tail. After the addition, the cyclopentadienyl ring loses its stability, which mainly arises from its five resonance structures, which are no longer available. This reaction is exothermic by 7.6 kcal mol^{-1}, and its energy barrier is 13.3 kcal mol^{-1}. The activation energy for the dissociation reaction of the linear adduct is 20 kcal mol^{-1}. This is illustrated in the diagram of Figure 3, where the enthalpy

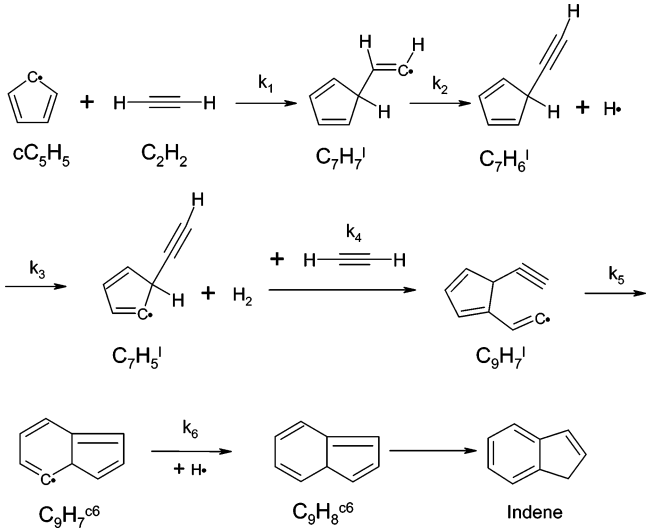

Figure 2. Kinetic pathway for the formation of $C_9H_8^{c6}$, which can be considered a precursor to indene, starting from the addition of acetylene and the cyclopentadienyl radical following the HACA mechanism.

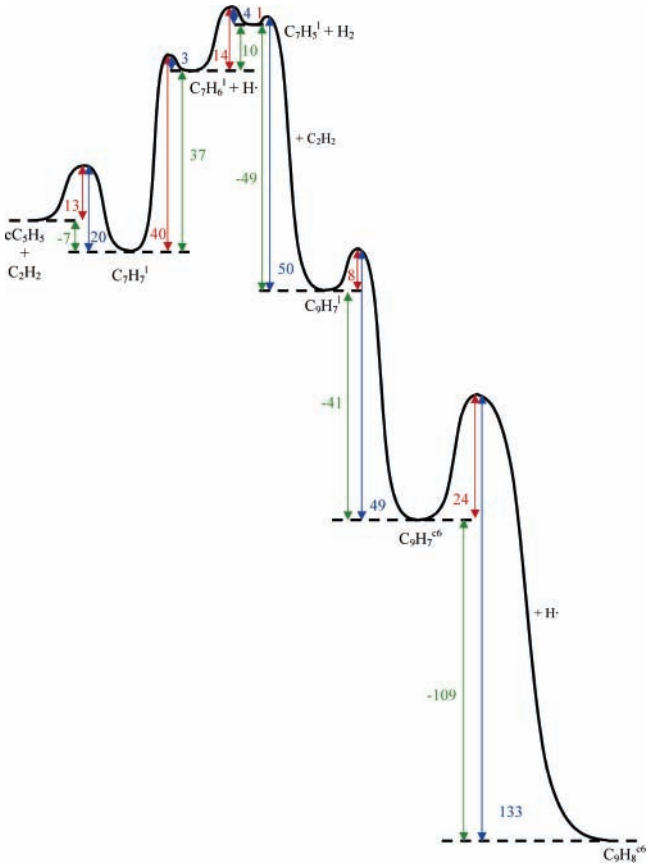

Figure 3. Activation energies (kcal mol^{-1}) for a possible kinetic pathway originated by the addition of C_2H_2 to cC_5H_5. The energies of the first reaction (which is common to the other pathways investigated) were calculated at the G2MP2* level of theory (see eq 2); the others were calculated at the B3LYP/6-31G(d,p) level and corrected with ZPE.

changes and activation energies of all the reactions involved in the kinetic scheme are reported.

However, the reaction entropy change is −31.08 cal mol^{-1} K^{-1}). That is indicative of a loss of stability by the C5 ring, which is reflected in the calculated preexponential factors: the backward reaction presents a frequency factor that at 2000 K is about 1 order of magnitude larger than that of the forward reaction: 2.1×10^{12} s^{-1} vs 3.2×10^{11} cm^3 mol^{-1} s^{-1}). The

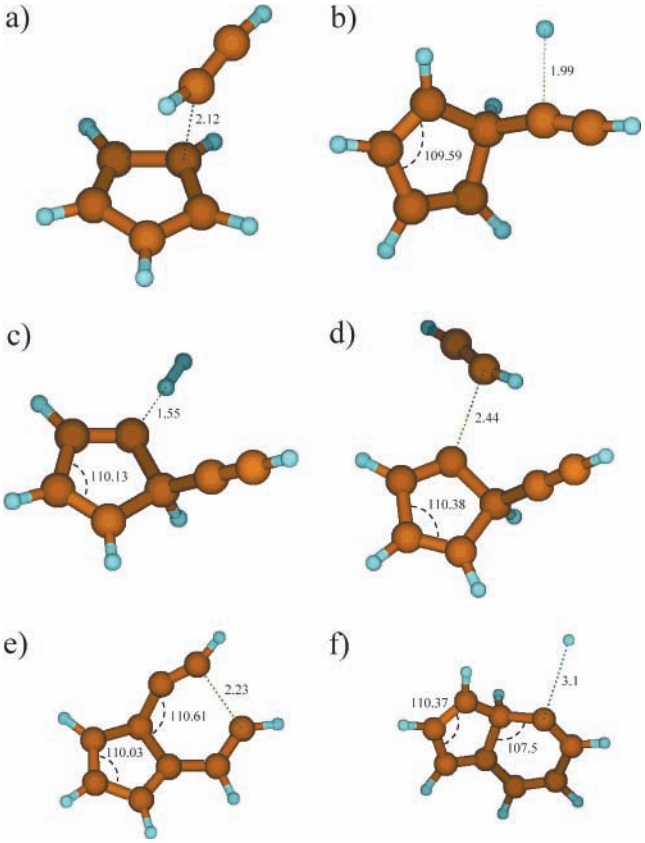

Figure 4. Transition state structures for the HACA reaction mechanism: (a) $cC_5H_5 + C_2H_2 \rightarrow C_7H_7^l$; (b) $C_7H_7^l \rightarrow C_7H_6^l + H$; (c) $C_7H_6^l + H \rightarrow C_7H_5^l + H_2$; (d) $C_7H_5^l + C_2H_2 \rightarrow C_9H_7^l$; (e) $C_9H_7^l \rightarrow C_9H_7^{c6}$; (f) $C_9H_7^{c6} + H \rightarrow C_9H_8^{c6}$. Distances are reported in Å and angles in deg.

cleavage of the carbon−carbon bond proceeds through a tight transition state, the C−C distance being 2.12 Å (see Figure 4a), which is much smaller than the 2.77 Å found for a similar reaction of dissociation of a single C−C bond, namely, that of dissociation of the butadiene−phenyl adduct.[27]

$C_7H_7^l$ can successively lose a hydrogen atom to form a stable compound, the $C_7H_6^l$ molecule: this step requires overcoming a high energy barrier, about 40 kcal mol^{-1}, mainly due to the reaction endothermicity, equal to 38.9 kcal mol^{-1}. Once formed, $C_7H_6^l$ can react again with atomic hydrogen to give the $C_7H_5^l$ radical or dissociate to give back the reactants. The reaction of hydrogen with $C_7H_6^l$ requires overcoming an energetic barrier of 13.5 kcal mol^{-1}, mainly determined by the endothermicity of the reaction (10.4 kcal mol^{-1}). The $C_7H_5^l$ radical successively reacts following the HACA mechanism with a second acetylene molecule. This reaction is very exothermic (50 kcal mol^{-1}), and the kinetic barrier that contrasts the addition of the two compounds is very low (1.4 kcal mol^{-1}), so the reaction proceeds rapidly at every temperature. The linear $C_9H_7^l$ adduct can then cyclize quickly, forming the indenyl radical. This reaction is significantly faster than the dissociation to the reactants, $C_7H_5^l$ and C_2H_2. At a temperature of 2000 K, the ratio between the kinetic constants k_4 and k_{-3}, reported in Table 1, which summarizes all the kinetic and thermodynamic parameters of the reaction investigated, is equal to about 400.

Also, it is interesting to observe that the C−C length in the transition state dissociation to $C_7H_5^l$ and C_2H_2 is greater than that found in the transition state of the dissociation reaction of the first adduct (2.12 vs 2.44 Å). This can be interpreted as indicative of the greater stability of the $C_9H_7^l$ radical with respect to the $C_7H_5^l$ radical, the bond energy between C_2H_2 and cC_5H_5 increasing from 7.6 kcal mol^{-1} (attachment of the first C_2H_2 molecule) to 50 kcal mol^{-1} (attachment of the second C_2H_2 molecule), and it is mainly due to the high stability of cC_5H_5, as previously discussed.

The reactions that follow the formation of $C_9H_7^l$ are strongly exothermic, meaning that, once formed, $C_9H_7^l$ can easily cyclize to form $C_9H_7^{c6}$ ($\Delta H_R = -41.6$ kcal mol^{-1}) and successively add a hydrogen radical to form $C_9H_8^{c6}$, which can form indene, transposing a hydrogen atom. In this last case, the reaction is even more strongly favored, the enthalpy change being equal to −110.3 kcal mol^{-1}. Alternatively $C_9H_7^{c6}$ can transpose a hydrogen atom from a tertiary C to form the very stable indenyl radical. Indeed it is likely that the reactivity of the $C_9H_7^{c6}$ is more complicated than that we examined. However we decided to limit the detail of investigation of this reaction pathway since the formation of the $C_9H_7^{c6}$ precursor, $C_7H_5^l$, which is the rate-determining step of this reaction mechanism, is very slow and thus indicates that the whole reaction pathway is unlikely to proceed at a significant rate, independently from the $C_9H_7^{c6}$ kinetics.

As previously mentioned, the thermodynamic and kinetic parameters for all the reactions involved in the HACA mechanism are reported in Table 1, while all the transition states for these reactions are shown in Figure 4. From the analysis of the energetics of this reaction mechanism, as summarized in Figure 3, it appears evident that the bottleneck, in terms of global rate of production of indene, is overcoming the 40 kcal mol^{-1} energetic barrier necessary for $C_7H_7^l$ to lose a hydrogen atom and form the $C_7H_6^l$ intermediate. Therefore, it is extremely likely that, once formed, $C_7H_7^l$ will prefer to dissociate back to cC_5H_5 and C_2H_2, which reaction has an activation energy of 19.5 kcal mol^{-1} and a high preexponential factor, rather than lose a hydrogen atom to form $C_7H_6^l$, which has an activation energy of 40 kcal mol^{-1} and a preexponential factor similar to that of the dissociation reaction. This is reflected by the QRRK rate constants calculated for the first part of the reaction mechanism, which correspond to the following reactions:

$$cC_5H_5 + C_2H_2 \rightleftarrows C_7H_7^l* \rightarrow C_7H_6^l + H$$

The calculated kinetic constant is reported as a function of temperature in Figure 5. Despite the high rate of formation of the excited complex $C_7H_7^l*$ (4×10^8 cm^3 mol^{-1} s^{-1} at 1000 K), the net rate of production of $C_7H_6^l$ is small, since $C_7H_7^l*$ prefers to dissociate back to reactants rather than decompose to the products. For the sake of comparison with experimental data, we can observe that the experimental kinetic constant for the production of C_7H_7 at 1000 K from C_2H_2 and cC_5H_5 is about 5×10^8, thus about 3 orders of magnitude larger than that calculated.

We can therefore conclude that cC_5H_5 is unlikely to form large PAH species following the HACA reaction mechanism. A further reason to disfavor this reaction mechanism is that it requires atomic H as a reactant to proceed to the next step. However it seems unlikely that in the experimental data simulated in this paper the atomic H concentration is sufficiently high to let bimolecular reactions proceed at a significant rate, the bath gas being He and the radical precursor being 1,3-C_4H_6.

3.2. Addition−Stabilization without Ring Opening. As previously discussed, the addition of acetylene to cC_5H_5 to form the $C_7H_7^l$ linear adduct is exothermic by 7 kcal mol^{-1} and requires an activation energy of 13.3 kcal mol^{-1}. However $C_7H_7^l$ is an extremely unstable radical species and likely to decompose back to cC_5H_5 and C_2H_2 rather than proceed to form heavier

TABLE 1: Reaction Enthalpy Changes (kcal mol^{-1}) Calculated at 298 K and 1 atm and TST Kinetic Parameters ($k = AT^{\alpha}$ exp($-E/(RT)$)) for the "HACA" Reaction Mechanism[a]

	HACA	ΔH_R	A_{forw}	α	$E_{a_{forw}}$	A_{back}	α	$E_{a_{back}}$
k_1	$cC_5H_5 + C_2H_2 \rightarrow C_7H_7^{l}$	−7.6	3.2×10^{11}	0	13.3	4.2×10^{15}	−1	19.5
k_2	$C_7H_7^{l} \rightarrow C_7H_6^{l} + H$	38.9	8.8×10^{12}	0	40.1	8.0×10^{12}	0	2.6
k_3	$C_7H_6^{l} + H \rightarrow C_7H_5^{l} + H_2$	10.4	1.6×10^{13}	0	13.5	3.2×10^{12}	0	3.7
k_4	$C_7H_5^{l} + C_2H_2 \rightarrow C_9H_7^{l}$	−50.0	1.7×10^{11}	0	1.4	2.7×10^{16}	−1	50.3
k_5	$C_9H_7^{l} \rightarrow C_9H_7^{c6}$	−41.6	8.9×10^{11}	0	8.2	1.6×10^{13}	0	48.5
k_6	$C_9H_7^{c6} + H \rightarrow C_9H_8^{c6}$	−110.3	1.7×10^{12}	0	24.4	1.1×10^{13}	0	133.26

[a] Kinetic parameters are reported in units consistent with kcal, s, mol, and cm. Energies were calculated at G2MP2 level, modified as described in the text, for the most important reaction, that is, the addition of cC_5H_5 to C_2H_2, and at B3LYP/6-31G(d,p) level for the other reactions. The rate coefficients of the backward reactions were determined through thermodynamic consistence.

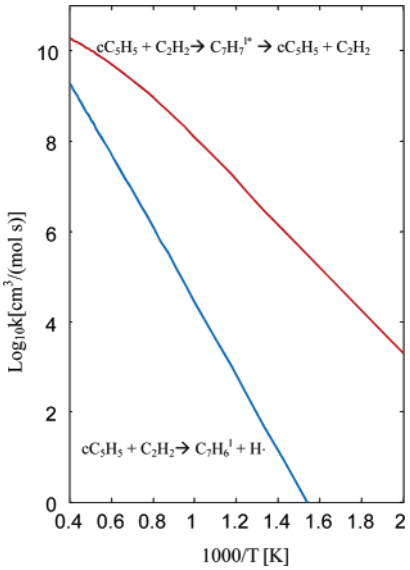

Figure 5. Results of the QRRK calculations performed at atmospheric pressure for the first part of the HACA mechanism leading to $C_7H_6^{l}$ from cC_5H_5 and C_2H_2 through the intermediate $C_7H_7^{l}$.

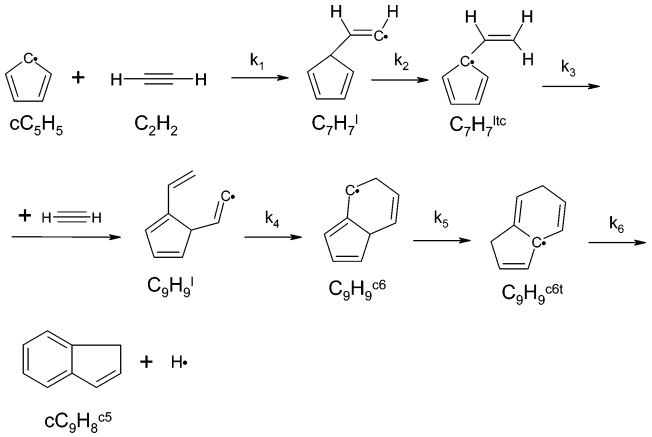

Figure 6. Kinetic pathway for the formation of indene following the addition of two molecules of acetylene to cyclopentadienyl radical (AcAc mechanism).

species. A possible alternative reaction pathway might consist in the transposition of a hydrogen atom from the cC_5H_5 to the acetylene tail (see Figure 6).

Through this transposition, the C_5 ring can recover the stability lost with the first reaction and, in particular, the resonance of the original cC_5H_5 radical structure. In fact, as shown in Table 2, where all the thermodynamic and kinetic parameters of the reactions involved in this mechanism are summarized, the hydrogen transposition reaction is exothermic by 45.1 kcal mol^{-1}, thus indicating that the new $C_7H_7^{ltc}$ can recover the stability of the cC_5H_5 parent species.

Also the activation energy of the successive reaction that is likely to take place, that is, the loss of a hydrogen atom, is smaller than that found in the HACA mechanism (27.5 vs 40.1 kcal mol^{-1}). Once formed and stabilized, $C_7H_7^{ltc}$ can then react with a second acetylene molecule and, through cyclization reactions, form a new C_6 ring. In the following, we will refer to this mechanism as the AcAc mechanism.

The addition of the second C_2H_2 to $C_7H_7^{ltc}$ follows a similar reaction pathway. The reaction is slightly endothermic (0.2 kcal mol^{-1}) and has an activation energy barrier higher than that of the first reaction (19.2 vs 13.3 kcal mol^{-1}) and a preexponential factor smaller by about 1 order of magnitude (4.8×10^{10} vs 3.1×10^{11} cm^3 mol^{-1} s^{-1}). The backward reaction has a relatively high preexponential factor of 2.0×10^{12} cm^3 mol^{-1} s^{-1} at 2000 K. Therefore, while the ratio between the backward and the forward reaction for the addition of C_2H_2 to C_5H_5 at 2000 K is equal to about 1.4, the corresponding ratio for the addition of C_2H_2 to $C_7H_7^{ltc}$ shows a value of nearly 50, clearly indicating that the activated complex is significantly unstable with respect to reactants.

The $C_9H_9^{l}$ intermediate is unstable and can give fast cyclization through the formation of a bond between the two acetylene tails, leading to a six carbon atom ring as evidenced in Figure 7.

This reaction is strongly exothermic (−49.7 kcal mol^{-1}), and the species so formed is thus energetically stabilized. Also the kinetic parameters evidence the fast rate of this reaction step: the ratio between the forward and the backward preexponential factors for obtaining $C_9H_9^{c6}$ and for giving back $C_7H_7^{ltc}$ and C_2H_2 at 2000 K is equal to about 0.3 (see Table 2), and the large difference between the energy barriers (3.7 vs 18.5 kcal mol^{-1}) makes the forward reaction favored. The ratio between the forward and the backward kinetic constants at 2000 K is equal to about 13. The successive reaction step, through which the molecule recovers the aromaticity, is the transposition of a hydrogen atom from the C_5H_5 sp^3 carbon atom, as shown in Figure 8d, which illustrates the transition state of this reaction (Figure 8 shows the transition states for all the reactions involved in this mechanism). The reaction is exothermic by 11.2 kcal mol^{-1} and the reaction of formation of $C_9H_9^{c6t}$ has a kinetic constant at 2000 K about 400 times larger than that of the backward reaction leading to $C_9H_9^{l}$.

Finally, the loss of a hydrogen atom from the second tertiary carbon atom leads to the formation of indene. In the HACA mechanism analyzed previously, the loss of the hydrogen atom leading to the formation of $C_7H_6^{l}$ requires about 39 kcal mol^{-1} (Table 1). However, in this case, the hydrogen loss is simultaneous with the recovery of the aromaticity, which decreases the endothermicity up to 24.6 kcal mol^{-1} (see Table 2). This corresponds to the decrease of the carbon−hydrogen distance in the transition state from 1.99 to 1.88 Å, which is consistent

TABLE 2: Reaction Enthalpy Changes (kcal mol^{-1}) Calculated at 298 K and 1 atm and TST Kinetic Parameters for the "AcAc" Reaction Mechanism[a]

	AcAc	ΔH_R	A_{forw}	α	$E_{a_{forw}}$	A_{back}	α	$E_{a_{back}}$
k_1	$cC_5H_5 + C_2H_2 \rightarrow C_7H_7^{l}$	−7.6	3.2×10^{11}	0	13.3	4.2×10^{15}	−1	19.5
k_2	$C_7H_7^{l} \rightarrow C_7H_7^{ltc}$	−45.1	3.1×10^{12}	0	27.5	4.8×10^{12}	0	72.5
k_3	$C_7H_7^{ltc} + C_2H_2 \rightarrow C_9H_9^{l}$	0.2	4.8×10^{10}	0	19.2	3.9×10^{15}	−1	18.5
k_4	$C_9H_9^{l} \rightarrow C_9H_9^{c6}$	−49.7	6.0×10^{11}	0	3.7	9.1×10^{13}	0	52.2
k_5	$C_9H_9^{c6} \rightarrow C_9H_9^{c6t}$	−11.2	5.1×10^{12}	0	25.1	4.9×10^{12}	0	36.3
k_6	$C_9H_9^{c6t} \rightarrow cC_9H_8^{c5} + H$	24.6	5.0×10^{12}	0	26.6	6.5×10^{12}	0	3.1

[a] Kinetic parameters are reported in units consistent with kcal, s, mol, and cm. Energies were calculated at G2MP2* level for the most important reaction, that is, the addition of cC_5H_5 to C_2H_2, and at the B3LYP/6-31G(d,p) level for the other reactions. The rate coefficients of the backward reactions were determined through thermodynamic consistence.

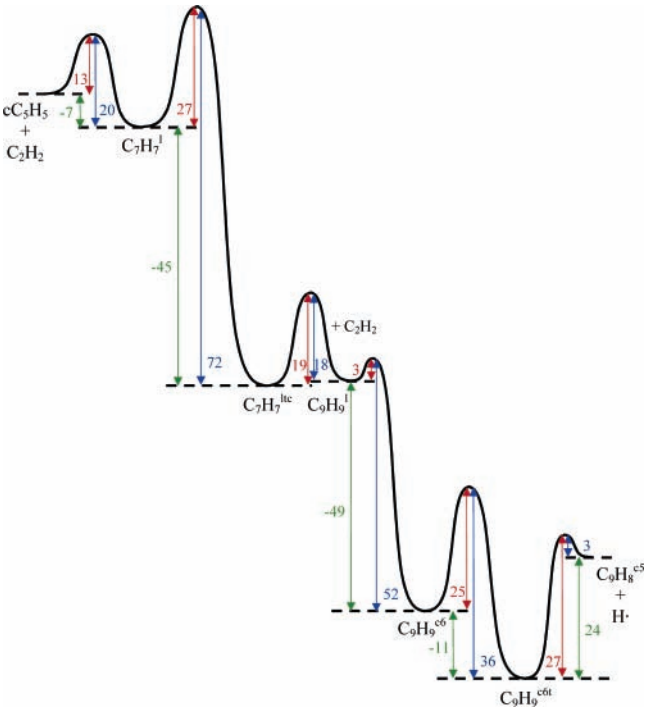

Figure 7. Activation energies for the second kinetic pathway proposed for the reactions that follow the addition of two C_2H_2 molecules to cC_5H_5 (kcal mol^{-1}). The energies of the first reaction (which is common to the other pathways investigated) were calculated at the G2MP2* level of theory (see eq 2); the others were calculated at the B3LYP/6-31G(d,p) level and corrected with ZPE.

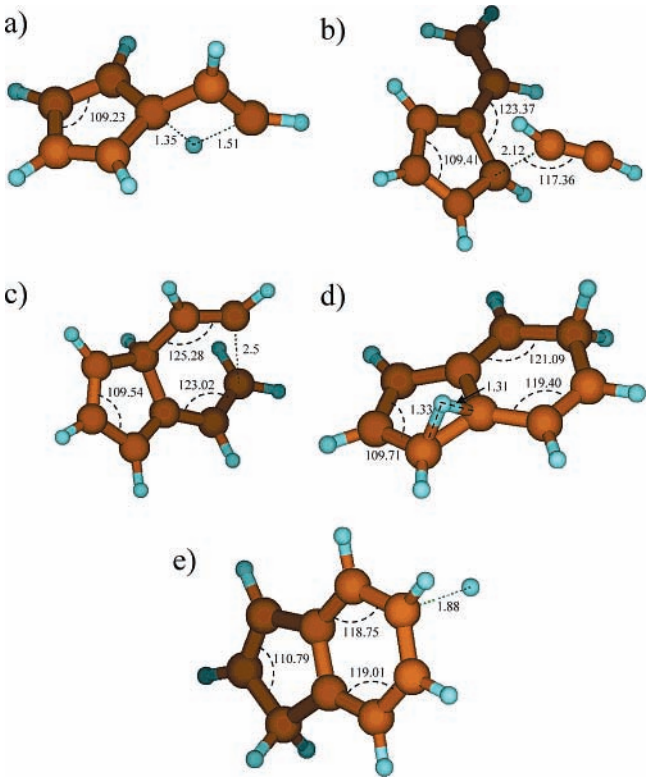

Figure 8. Transition state structures for the AcAc reaction mechanism: (a) $C_7H_7^{l} \rightarrow C_7H_7^{ltc}$; (b) $C_7H_7^{ltc} + C_2H_2 \rightarrow C_9H_9^{l}$; (c) $C_9H_9^{l} \rightarrow C_9H_9^{c6}$; (d) $C_9H_9^{c6} \rightarrow C_9H_9^{c6t}$; (e) $C_9H_9^{c6t} \rightarrow cC_9H_8^{c5} + H$. Distances are reported in Å and angles in deg.

with overcoming an energetic barrier smaller than that involved in the other reaction.

Similar to what was done previously, the global rate constant for the formation of C_7H_7 was calculated using QRRK theory according to the following reaction scheme:

$$cC_5H_5 + C_2H_2 \rightleftarrows C_7H_7^{l}* \rightleftarrows C_7H_7^{ltc}* \xrightarrow{\beta ZM} C_7H_7^{ltc}$$

The calculate kinetic constant for the formation of $C_7H_7^{ltc}$ is reported, together with the rate of dissociation of the excited complex back to reactants, in Figure 9.

Also in this case the excited complex $C_7H_7^{l}*$ prefers to dissociate back to the reactants rather than form the $C_7H_7^{ltc}$ species. In particular at 1000 K, the kinetic constant is still 2 orders of magnitude smaller than that experimentally measured, thus showing that the C_2H_2 addition pathway is different from that here discussed.

3.3. Addition−Stabilization with Ring Opening. *First Step: The Addition of C_2H_2 to cC_5H_5.* The two mechanisms analyzed in the previous paragraphs seem to confirm the general view that cC_5H_5 is a very stable molecule that is unlikely to give addition−cyclization reactions, except when reacting with another cC_5H_5 radical.[14] From the detailed kinetic analysis performed above, we found that this lack of reactivity can be traced back to the fact that the energy stabilization due to the addition of C_2H_2 is not sufficient to compensate for the loss of entropy determined by the freezing of the translational and rotational degrees of freedom of C_2H_2. However the experimental evidence discussed in the Introduction clearly indicated that, even at a relatively low temperature of 1000 K, cC_5H_5 and C_2H_2 could react rapidly to form a C_7H_7 stable intermediate. We therefore decided to investigate what, at the beginning, seemed to be a pretty improbable reaction pathway: the opening of the cC_5H_5 ring and the insertion of C_2H_2 leading to a seven atom ring. As evidenced by our previous calculations, the reason all the reactions investigated could not proceed at a significant rate was that they require the formation of very unstable intermediates. Therefore we hypothesized that, following the C_2H_2 addition and the formation of $C_7H_7^{l}$, the tail of C_2H_2, on which an unpaired electron is located, could react with a neighboring C atom of the C_5 ring to form a four-membered ring, namely, $C_7H_7^{c4}$, as shown in Figure 10. The formation of a bicyclic intermediate species involving from three-membered

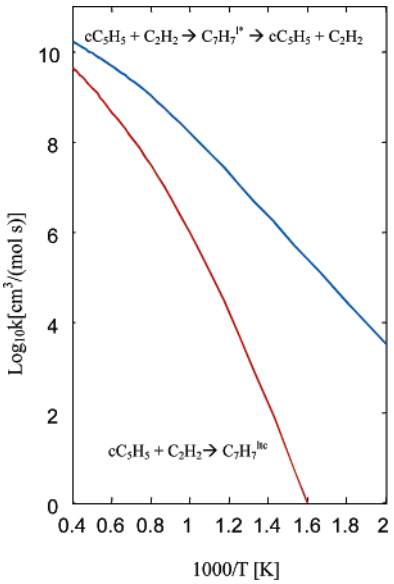

Figure 9. Results of the QRRK calculation performed at atmospheric pressure for the first part of the AcAc mechanism leading to $C_7H_7^{ltc}$ from cC_5H_5 and C_2H_2 through the $C_7H_7^{l*}$ and $C_7H_7^{ltc*}$ intermediates.

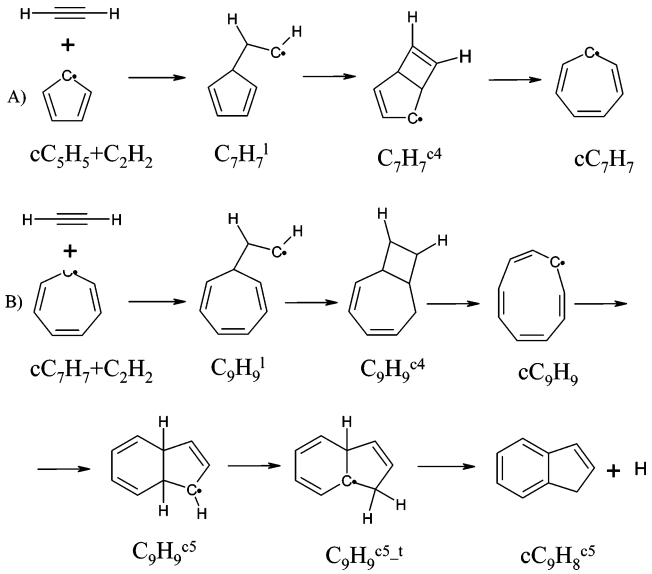

Figure 10. Third kinetic pathway proposed for the formation of indene following the addition of acetylene to cC_5H_5, in which the heptatrienyl radical appears as an intermediate (C_7 mechanism).

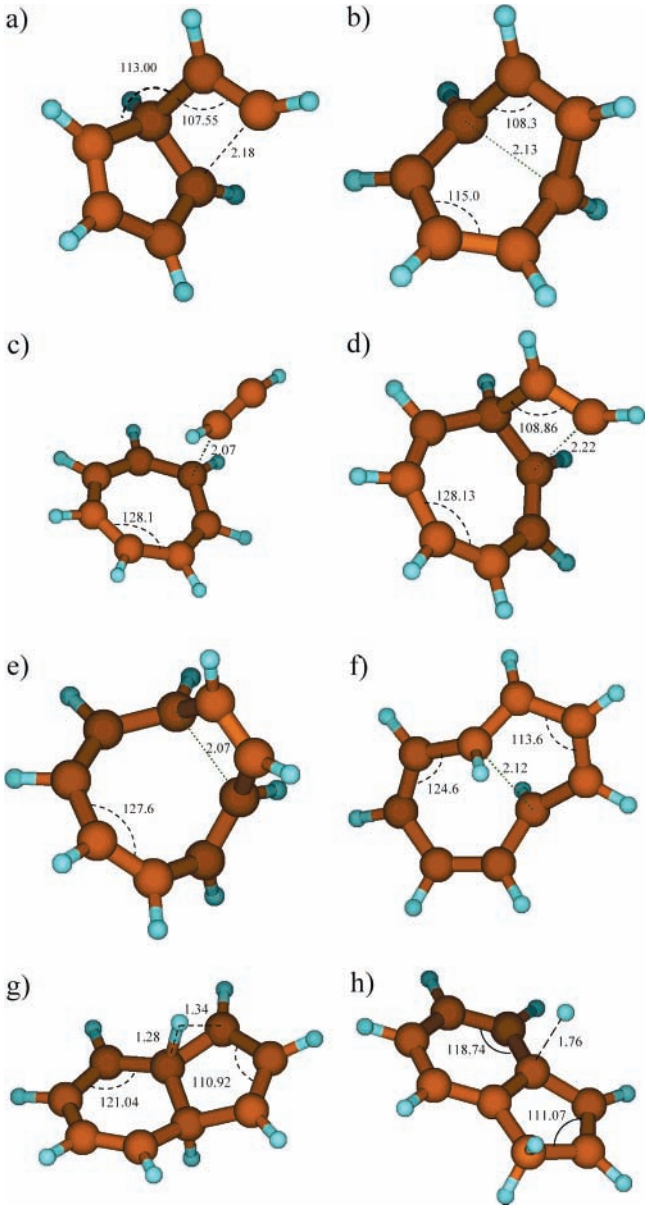

Figure 11. Transition state structures for the C_7 reaction mechanism: (a) $C_7H_7^{l} \rightarrow C_7H_7^{c4}$; (b) $C_7H_7^{c4} \rightarrow C_7H_7$; (c) $cC_7H_7 + C_2H_2 \rightarrow C_9H_9^{l}$; (d) $C_9H_9^{l} \rightarrow C_9H_9^{c4}$; (e) $C_9H_9^{c4} \rightarrow C_9H_9$; (f) $C_9H_9 \rightarrow C_9H_9^{c5}$; (g) $C_9H_9^{c5} \rightarrow C_9H_9^{c5-t}$; (h) $C_9H_9^{c5-t} \rightarrow cC_9H_8^{c5} + H$. Distances are reported in Å and angles in deg.

up to seven-membered or more rings has in fact been proposed to describe the reactivity of several hydrocarbon radicals, as well as peroxyradicals (e.g., cC_7H_8,[22] $cC_5H_5 + cC_5H_5$[2]). The transition state of this reaction is reported in Figure 11a, together with those of the other reactions involved in this mechanism, in the following referred to as the C_7 mechanism. $C_7H_7^{c4}$ is a bicyclic nonplanar molecule with an angle between the planes of the two cycles of 113°.

Despite the internal strain, the formation of the C_4 ring is exothermic by 16.1 kcal mol^{-1}. This means that $C_7H_7^{c4}$ is more stable than the initial reactants by about 23 kcal mol^{-1}. The energetics of the formation of cycloheptatrienyl via addition of cyclopentadienyl to acetylene is shown in Figure 12. The energy barriers of the first and the second forward reactions are about 13 kcal mol^{-1}, while the activation energy of the backward reaction, corresponding to the opening of the C_4 ring, is particularly high (28.7 kcal mol^{-1}). Also the preexponential factors differ by about 1 order of magnitude. Consequently, $C_7H_7^{c4}$ is a relatively stable product with respect to dissociation into cC_5H_5 and C_2H_2. In fact, the ratio between the rate of formation of $C_7H_7^{c4}$ starting from $C_7H_7^{l}$ and that of dissociation to cC_5H_5 and C_2H_2 at 2000 K is equal to about 10 and increases as the temperature decreases. The kinetic and thermodynamic parameters for this reaction pathway are reported in Table 3.

The bicyclic compound $C_7H_7^{c4}$ is an interesting chemical species, the stability of which arises from being a radical species with the unpaired electron delocalized on the C_5 ring. However, though energetically favored with respect to the reactants, $C_7H_7^{c4}$ has a large internal strain, only partially compensated by the sp^3 hybridization of the two C atoms shared by the two rings. A possibility for $C_7H_7^{c4}$ to accommodate its internal strain and therefore proceed toward a more stable state is to break the bond between the two sp^3 C atoms and form the cycloheptatrienyl radical (cC_7H_7).

As reported in Figure 12, the cycloheptatrienyl radical is highly energetically stabilized with respect to the starting

TABLE 3: Reaction Enthalpy Changes (kcal mol^{-1}) Calculated at 298 K and 1 atm and TST Kinetic Parameters ($k = AT^{\alpha}\exp(-E/(RT))$) for the C_7 Reaction Mechanism[a]

B3LYP/6-31G(d,p)

	reaction	ΔH_R	A_{forw}	α	$E_{a_{forw}}$	A_{back}	α	$E_{a_{back}}$
k_1	$cC_5H_5 + C_2H_2 \rightarrow C_7H_7{}^{l}$	−7.2	3.2×10^{11}	0	12.9	4.2×10^{15}	−1	18.7
k_2	$C_7H_7{}^{l} \rightarrow C_7H_7{}^{c4}$	−17.3	3.1×10^{12}	0	10.4	1.6×10^{13}	0	27.1
k_3	$C_7H_7{}^{c4} \rightarrow cC_7H_7$	−33.8	1.4×10^{13}	0	24.6	2.7×10^{13}	0	59.0
k_4	$cC_7H_7 + C_2H_2 \rightarrow C_9H_9{}^{l}$	3.8	1.2×10^{12}	0	20.4	7.5×10^{15}	−1	15.3
k_5	$C_9H_9{}^{l} \rightarrow C_9H_9{}^{c4}$	−19.7	6.7×10^{12}	0	11.0	1.8×10^{13}	0	30.2
k_6	$C_9H_9{}^{c4} \rightarrow cC_9H_9$	−6.7	1.3×10^{13}	0	24.6	2.4×10^{11}	0	31.9
k_7	$cC_9H_9 \rightarrow C_9H_9{}^{c5}$	−4.3	1.1×10^{11}	0	31.3	7.7×10^{12}	0	34.8
k_8	$C_9H_9{}^{c5} \rightarrow C_9H_9{}^{c5-t}$	−17.6	5.9×10^{12}	0	28.9	4.1×10^{12}	0	46.5
k_9	$C_9H_9{}^{c5-t} \rightarrow cC_9H_8{}^{c5} + H$	14.7	4.5×10^{12}	0	20.5	5.5×10^{12}	0	7.0

G2MP2

	reaction	ΔH_R	A_{forw}	α	$E_{a_{forw}}$	A_{back}	α	$E_{a_{back}}$
k_1	$cC_5H_5 + C_2H_2 \rightarrow C_7H_7{}^{l}$	−7.6	3.2×10^{11}	0	13.3	4.2×10^{15}	−1	19.5
k_2	$C_7H_7{}^{l} \rightarrow C_7H_7{}^{c4}$	−16.1	3.1×10^{12}	0	13.2	1.6×10^{13}	0	28.7
k_3	$C_7H_7{}^{c4} \rightarrow cC_7H_7$	−25.7	1.4×10^{13}	0	26.6	2.7×10^{13}	0	52.9
k_4	$cC_7H_7 + C_2H_2 \rightarrow C_9H_9{}^{l}$	−1.3	1.2×10^{12}	0	20.1	7.5×10^{15}	−1	20.1
k_5	$C_9H_9{}^{l} \rightarrow C_9H_9{}^{c4}$	−15.3	6.7×10^{12}	0	17.1	1.8×10^{13}	0	31.9
k_6	$C_9H_9{}^{c4} \rightarrow cC_9H_9$	−1.5	1.3×10^{13}	0	23.5	2.4×10^{11}	0	25.6
k_7	$cC_9H_9 \rightarrow cC_9H_9{}^{c5}$	−14.6	1.1×10^{11}	0	26.8	7.7×10^{12}	0	40.5
k_8	$C_9H_9{}^{c5} \rightarrow C_9H_9{}^{c5-t}$	−14.1	5.9×10^{12}	0	33.6	4.1×10^{12}	0	47.8
k_9	$C_9H_9{}^{c5-t} \rightarrow cC_9H_8{}^{c5} + H$	12.6	4.5×10^{12}	0	23.7	5.5×10^{12}	0	11.6

[a] Kinetic parameters are reported in units consistent with kcal, s, mol, and cm. All calculations were performed both at the B3LYP/6-31G(d,p) and G2MP2* levels of theory. The rate coefficients of the backward reactions were determined through thermodynamic consistence.

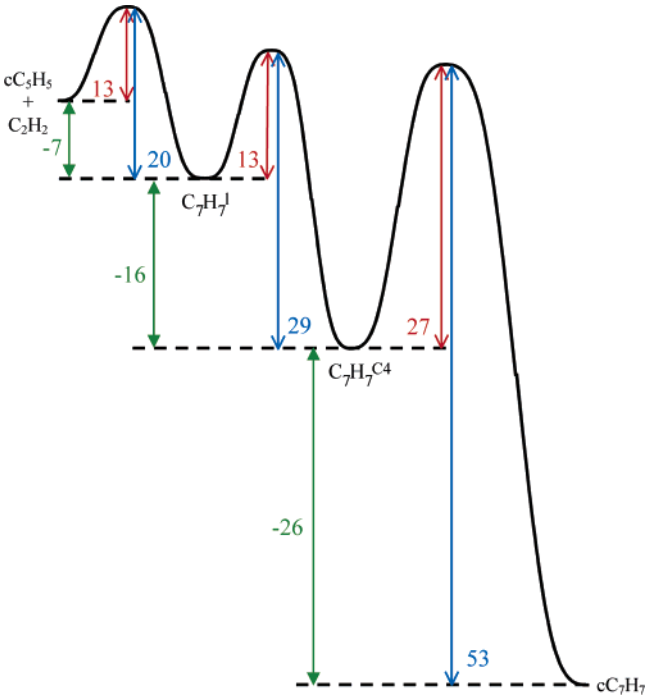

Figure 12. Activation energies for the kinetic pathway following the reaction of addition of C_2H_2 to cC_5H_5 and resulting in the formation of the cycloheptatrienyl radical (kcal mol^{-1}). All energies were calculated at the G2MP2* level, as specified in eq 2.

cyclopentadienyl and acetylene reactants (−49.4 kcal mol^{-1}). The cycloheptatrienyl radical is, in many ways, similar to the cyclopentadienyl radical. They are both characterized by large rotational symmetry numbers, 14 and 10, respectively, the radical center is delocalized on the whole molecule, and the geometries of both molecules are distorted by the Jahn−Teller effect[1]. Finally, they both have one electron in excess (cC_7H_7) or in defect (cC_5H_5) for becoming aromatic. Their respective cations and anions are in fact well-known in organic chemistry and extensively used as complexants. It appears thus as an

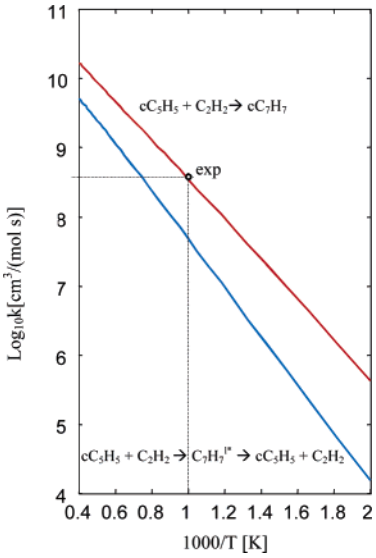

Figure 13. Results of the QRRK calculations performed at atmospheric pressure for the first part of the C_7 mechanism, leading to the formation of cycloheptatrienyl from cyclopentadienyl and acetylene. The reported experimental data is that measured at 1000 K for the reaction $cC_5H_5 + C_2H_2 \rightarrow C_7H_7$.[20]

interesting possibility that the reaction between cC_5H_5 and C_2H_2 might result in the formation of what can be considered the superior homologue to cC_5H_5, the cycloheptatrienyl radical.

Also in this case, the kinetic constant for the global reaction leading to the production of cycloheptatrienyl from cyclopentadienyl and acetylene was calculated using QRRK theory according to the following reaction scheme:

$$cC_5H_5 + C_2H_2 \rightleftarrows C_7H_7{}^{l*} \rightleftarrows C_7H_7{}^{c4*} \xrightarrow{\beta zm} \begin{matrix} cC_7H_7 \\ C_7H_7{}^{c4} \end{matrix}$$

The calculated rate constant for the formation of cC_7H_7 is reported in Figure 13 as a function of temperature, together with that of the dissociation of the excited complex $C_7H_7{}^{l*}$ back to the reactants. Different from what was found for the first two

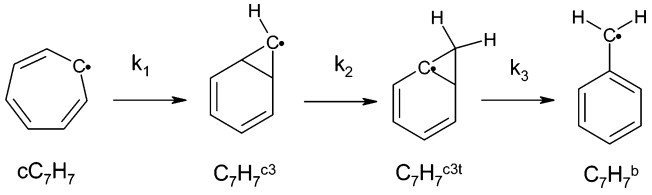

Figure 14. A possible reaction pathway for the conversion of cC_7H_7 into the benzyl radical.

investigated reaction mechanisms, there are no bottlenecks in this succession of reactions, the rate of dissociation of the excited complex being smaller than that of formation of cC_7H_7.

The calculated overall rate constant for the formation of cC_7H_7 starting from cC_5H_5 and C_2H_2 can be directly compared with that experimentally measured by Knyazev and Slagle at 1000 K.[20] Even if the authors report only a pseudo-first-order kinetic constant, which means that it includes the C_2H_2 concentration, the bimolecular rate constant can be obtained by dividing the reported value by the C_2H_2 concentration used in the experiment. The experimental and calculated values are 5.2×10^8 and 3.5×10^8 cm^3 mol^{-1} s^{-1}, respectively. This good agreement between experiment and theory (also evidenced in Figure 13) seems to indicate that the C_7H_7 species observed by Knyazev and Slagle could be the cycloheptatrienyl radical. This is one of the most interesting findings of this work since, up to now, to our knowledge it was not known that cC_7H_7 could be produced at relatively low temperatures and high rate through the addition of C_2H_2 to cC_5H_5. This finding can also be of some relevance for combustion studies, since, as previously mentioned, cC_5H_5 and C_2H_2 are often among the most abundant radicals and stable hydrocarbon species present in a flame. Therefore the formation of an intermediate cyclic species containing a ring of seven atoms might be an important kinetic pathway, till now unexplored, for the growth of low molecular weight hydrocarbons, eventually leading to the formation of PAHs and soot.

The kinetic constant values computed with QRRK theory for the overall reaction $cC_5H_5 + C_2H_2 \rightarrow cC_7H_7$ have been interpolated in the range 500−2500 K, leading to $k_{C7} = (2.2 \times 10^{11})\exp(-6440/T(\mathrm{K}))$ cm^3 mol^{-1} s^{-1}. The corresponding backward kinetic constant values have been calculated, enforcing the thermodynamic consistence; interpolating these data results in the relation $k_{C7-} = (4.2 \times 10^{16})T^{-1} \exp(-30\,850/T(\mathrm{K}))$ s^{-1}.

Apart from the pathway sketched in Figure 10, it is also interesting to explore other possible reaction pathways that might follow the formation of cC_7H_7. First of all, since cC_7H_7 is an isomer of the benzyl radical, $C_7H_7^b$, which is thermodynamically more stable by about 16 kcal mol^{-1}, we investigated the interconversion of the two chemical species. The reaction pathway that we investigated is shown in Figure 14 and mimics that proposed to describe the conversion of cycloheptatriene into toluene previously discussed and summarized in Figure 1.

The energetics of this reaction pathway was calculated using density functional theory at the B3LYP/6-31G(d,p) level and is reported in Figure 15. The first reaction is the formation of the norcaradienyl radical ($C_7H_7^{c3}$), a bycyclic species formed by two rings of six and three carbon atoms, respectively. From the thermodynamic analysis, reported in Table 4, together with the kinetic parameters for all the considered reactions, this first step appears to be significantly endothermic (45.2 kcal mol^{-1}). The activation energy for the formation of $C_7H_7^{c3}$ is close to the reaction enthalpy, 45.4 kcal mol^{-1}. The next step is the transposition of a hydrogen atom from the C_3 ring to the C_6 ring leading to the $C_7H_7^{c3t}$ species. This reaction is exothermic

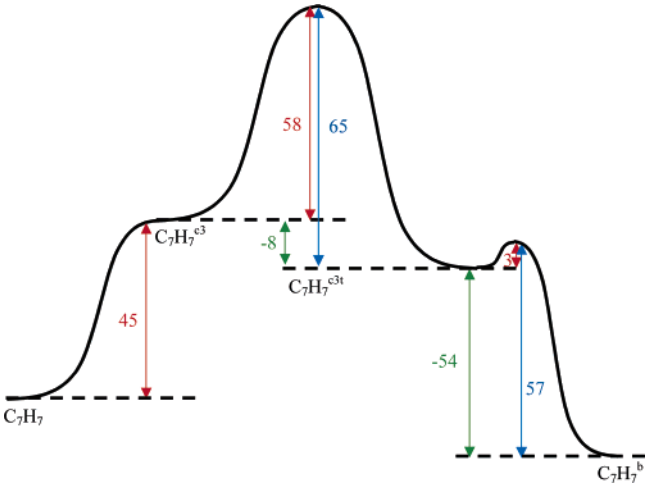

Figure 15. Calculated activation energies for the kinetic pathway sketched in Figure 14 describing the conversion of cC_7H_7 into the benzyl radical (kcal mol^{-1}). All values were determined at the B3LYP/6-31G(d,p) level and corrected with ZPE.

TABLE 4: Reaction Enthalpy Changes (kcal mol^{-1}) Calculated at 298 K and 1 atm and TST Kinetic Parameters ($k = AT^{\alpha} \exp(-E/(RT))$) for the Conversion of cC_7H_7 into the Benzyl Radical[a]

	reaction	ΔH_R	A_{forw}	α	$E_{a_{forw}}$	A_{back}	α	$E_{a_{back}}$
k_1	$cC_7H_7 \rightarrow C_7H_7^{c3}$	45.2	2.4×10^{13}	0	45.4	4.7×10^{12}	0	0
k_2	$C_7H_7^{c3} \rightarrow C_7H_7^{c3t}$	−7.7	6.7×10^{12}	0	57.7	5.9×10^{12}	0	65.3
k_3	$C_7H_7^{c3t} \rightarrow C_7H_7^{b}$	−53.9	4.2×10^{12}	0	2.8	4.6×10^{12}	0	56.7

[a] Kinetic parameters are reported in units consistent with kcal, s, mol, and cm. Energies were calculated at B3LYP/6-31G(d,p) level. The rate coefficients of the backward reactions were determined through thermodynamic consistence.

by about 7.7 kcal mol^{-1}, but its activation barrier is much higher, 57.7 kcal mol^{-1}. The $C_7H_7^{c3t}$ species is very unstable since, while the energetic barrier to decompose back to the norcaradienyl radical is high (65 kcal mol^{-1}), that required to produce the benzyl radical is small (2.8 kcal mol^{-1}).

An interesting comparison can be made with the aforementioned reaction mechanism proposed to describe the internal rearrangement of cycloheptatriene to toluene (C_7H_8). Its first step is the conversion of cycloheptatriene to norcaradiene, which is analogous to the first reaction of the mechanism shown in Figure 14, namely, the conversion of the cycloheptatrienyl radical into the norcaradienyl radical. However, while for the cycloheptatriene the reaction is exothermic by 6.6 kcal mol^{-1} with an activation energy equal to only 9.4 kcal mol^{-1}, in the case of the cycloheptatrienyl radical the enthalpy change, calculated at the same level of theory (B3LYP/6-31G(d,p)), is endothermic and equal to 45.2 kcal mol^{-1}. An alternative reaction mechanism for the formation of the benzyl radical from cC_7H^7 consists of the transposition of the H atom followed by the formation of the bicyclic intermediate. The H transposition reaction, investigated at the B3LYP/6-31G(d,p) level, is endothermic by 38.5 kcal mol^{-1} and has an activation energy of 80.1 kcal mol^{-1}. Though this second mechanism is energetically favored with respect to that sketched in Figure 15, the energetic barrier appears still to be too high to let this reaction proceed at a significant rate.

The second step involved in the cycloheptatriene mechanism, the H transposition to form an unstable byradical species, which quickly converts to toluene, has an activation energy of 43.15 kcal mol^{-1}. Also this value is significantly smaller than that calculated for the corresponding benzyl formation reaction, 57.7

kcal mol^{-1}. On the basis of these results, we can conclude that the conversion of cC_7H_7 to the benzyl radical is prohibited, at least for the reaction mechanism that we investigated, by a very high energetic barrier. However cC_7H_7 might be converted to benzyl radical through a bimolecular reaction with atomic hydrogen, which would result in the formation of cycloheptatriene, whic, as discussed previously, can be converted to toluene following the reaction mechanism outlined in Figure 14. Toluene, losing a hydrogen atom, can then form benzyl.

As a final remark, it is interesting to observe that, if cC_7H_7 is formed in flames following the above proposed mechanism, it is then possible that a portion of the C_7H_7 signal measured in flames and usually attributed to the benzyl radical is instead determined by cC_7H_7 radicals. Further experimental investigations are clearly required to elucidate this point.

Second Step: The Addition of C_2H_2 to cC_7H_7. The final step of our investigation was the study of the reaction between cC_7H_7 and C_2H_2. Having the same molecular structure of cC_5H_5, it is likely that cC_7H_7 reacts with C_2H_2 following a reaction pathway similar to the one described in the previous paragraph for the formation of the cycloheptatrienyl radical. In particular, the transition state for the addition of C_2H_2 to cC_7H_7 to give $C_9H_9^{l}$ is illustrated in Figure 11c. It can be observed that the carbon−carbon distance along the reaction coordinate is smaller than that calculated for the $cC_5H_5-C_2H_2$ addition (2.07 vs 2.12 Å) and that the reaction is exothermic only by −1.3 kcal mol^{-1}, versus −7.6 kcal mol^{-1} calculated for the addition of C_2H_2 to cC_5H_5. The kinetic parameters reported in Table 3 reflect this situation: even if the preexponential factors for the two reactions are similar (3.2×10^{11} vs 2.7×10^{11} cm^3 mol^{-1} s^{-1}), a clear difference is evident in the activation energies (13.3 vs 20.1 kcal mol^{-1}). Also the analysis of the next reaction giving $C_9H_9^{c4}$ shows a lower kinetic constant with respect to the analogous formation reaction of $C_7H_7^{c4}$: once more, the preexponential factors are comparable, 3.3×10^{12} vs 3.1×10^{12} s^{-1}, but the energy barrier is greater, 13.2 vs 17.1 kcal mol^{-1}. Consequently, the kinetic constant calculated at 2000 K for the formation of $C_9H_9^{c4}$ is about 2.5 times lower than that previously obtained for the formation of $C_7H_7^{c4}$.

The opening of the carbon−carbon bond to give cC_9H_9 follows a kinetics comparable to that of the formation of cC_7H_7; in fact, while the activation energy for the formation of the cC_9H_9 is lower than that for the formation of cC_7H_7 (23.5 vs 26.6 kcal mol^{-1}), the preexponential factor is slightly smaller (6.6×10^{12} vs 1.4×10^{13} s^{-1})). Consequently, at 2000 K the reaction of production of cC_9H_9 from $C_9H_9^{c4}$ has a kinetic constant equal to 1.8×10^{10} s^{-1}, which is very similar to the value of 1.7×10^{10} s^{-1} calculated for the formation of cC_7H_7 from $C_7H_7^{c4}$.

The structure of the cC_9H_9 radical is that of a ring formed by nine carbon atoms and, similarly to cC_5H_5 and cC_7H_7, stabilized by nine resonant structures. However, with respect to cC_5H_5 and cC_7H_7, the molecule is no longer planar but is slightly distorted. The reaction of formation of cC_9H_9 is endoentropic by 8.5 cal mol^{-1} K^{-1} and exothermic by 1.5 kcal mol^{-1}. This large ring is unlikely to be stable and can react rapidly following several reaction pathways. The energetically favored pathway involves the formation of a carbon−carbon bond to obtain a new chemical compound $C_9H_9^{c5}$, characterized by two rings of six and five carbon atoms respectively, which structure is sketched in Figure 10. The reaction energetics, reported in Table 3, is also sketched in Figure 16.

The formation of $C_9H_9^{c5}$ is thermodynamically favored (−14.6 kcal mol^{-1}), and its kinetic parameters are comparable

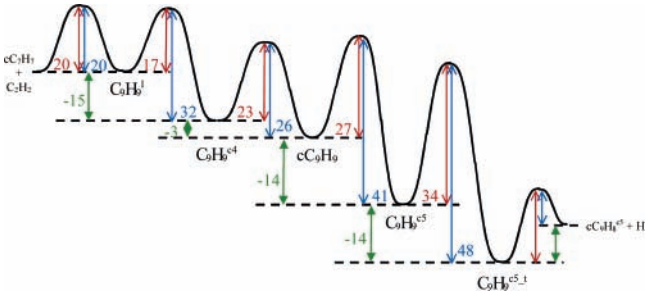

Figure 16. Activation energies for the kinetic pathway following the addition of C_2H_2 to cC_7H_7 to give the nonadienyl radical (kcal mol^{-1}). All energies were calculated at the G2MP2* level of theory, as specified in eq 2.

with that found for its decomposition into $C_9H_9^{c4}$: the rate of decomposition at 2000 K is 3 times faster than that of the formation of the double ring (3.8×10^8 vs 1.3×10^8 s^{-1}). The next reaction involves a hydrogen transposition leading to $C_9H_9^{c5-t}$, which is more stable than $C_9H_9^{c5}$ by 14.1 kcal mol^{-1}.

Finally, $C_9H_9^{c5-t}$ can lose a hydrogen atom to form indene. The transition state of this reaction is reported in Figure 11h. As in the case of the last reaction of the AcAc mechanism, discussed in the previous paragraph (see Table 2), this step is favored by the recover of the aromaticity by the six carbon atom ring. Therefore, even if endothermic, the value of the reaction enthalpy for this step is much lower than that involved in the AcAc mechanism (12.6 vs 24.6 kcal mol^{-1}). At 2000 K, the ratio between the rate of formation of indene from $C_9H_9^{c5-t}$ and that of the backward decomposition reaction of $C_9H_9^{c5-t}$ to $C_9H_9^{c5}$ is equal to about 500, showing that once formed $C_9H_9^{c5-t}$ decomposes rapidly into indene and hydrogen. This finding is in agreement with the investigation of the PES of C_9H_9 performed by Vereecken et al., who found that indene can be one of the principal products of the reaction between phenyl and propyne.[36]

The overall rate constant for the formation of indene from cycloheptatrienyl and acetylene was calculated with QRRK theory according to the following reaction scheme:

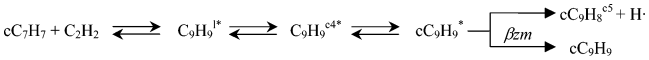

To simplify the QRRK calculations, the last three reactions of Table 3, corresponding to the conversion of $C_9H_9^{c5}$ into cC_9H_8, were lumped into a single reaction step. The results are reported in Figure 17 in terms of overall kinetic constant values as a function of temperature.

The overall kinetic constant values for the reaction $cC_7H_7 + C_2H_2 \rightarrow cC_9H_8^{c5}$ interpolated in the range 500−2500 K lead to the relation $k_{C9} = (6.6 \times 10^{11})\exp(-10\,080/T(\mathrm{K}))$ cm^3 mol^{-1} s^{-1}. The corresponding backward kinetic constant, calculated enforcing the thermodynamic consistence, is $k_{C9-} = (4.2 \times 10^{14})\exp(-27\,300/T(\mathrm{K}))$ cm^3 mol^{-1} s^{-1}.

The overall rate of production of $cC_9H_8^{c5}$ from cC_7H_7 and C_2H_2 is slower than that of formation of cC_7H_7 from cC_5H_5 and C_2H_2. As previously mentioned, this is essentially determined by the smaller thermodynamic stability of the intermediate adduct, cC_9H_9, with respect to cC_7H_7. The experimental production rate of indene, measured experimentally at 1000 K, was 3.4×10^8 cm^3 mol^{-1} s^{-1}, while the calculated value is 2.8×10^7 cm^3 mol^{-1} s^{-1}. This underestimation can be determined either by a different reaction pathway for the formation of $cC_9H_8^{c5}$ not considered in this work, by an error in the theoretical calculations, or by an overestimation of the experimental rate

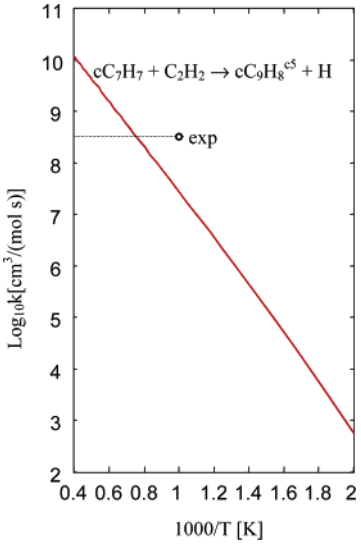

Figure 17. Results of the QRRK calculation for the second part of the C_7 mechanism leading to the formation of indene from cycloheptatrienyl and acetylene. The experimental data is that measured at 1000 K for the reaction $C_7H_7 + C_2H_2 \rightarrow C_9H_8 + H^{\bullet}$.[20]

constant from the experimental data fitting. The latter hypothesis is possible since the $C_9H_8^+$ mass spectroscopic signal did not show any plateau, as was the case for the $C_3H_3^+$, $C_5H_5^+$, and $C_7H_7^+$ signals. This makes it more difficult to extract quantitative information through the experimental data fitting, thus reducing the reliability of the overall reaction rate values with respect to that related to the formation of C_7H_7 species. Alternatively the disagreement between experimental and calculated data might be explained by an error of 4.5 kcal mol^{-1} in the calculated activation energies, which is however significantly larger than the mean error of G2MP2* calculations (2 kcal mol^{-1}).

Conclusions

In this work, the reactivity of cyclopentadienyl radical with respect to C_2H_2 has been investigated with the aim of increasing the knowledge on the kinetic pathways leading to the formation of PAHs and soot in combustion processes. The motivation for the work arose from some experimental measurements that evidenced the capability of cC_5H_5 to react with C_2H_2 leading in sequence to C_7H_7 and C_9H_8, the structure of these species being unknown.

Several reaction pathways have been investigated in this work through quantum chemistry and QRRK theory. It has been found that the classical addition of C_2H_2 to cC_5H_5 followed by the closure to the six atom ring on the two C_2H_2 tails cannot explain the experimental evidence related to the rate of formation of C_7H_7. This is mainly due to the high stability of cC_5H_5, which is completely lost as the reactions proceed.

A new pathway able to account for the experimental findings involving the insertion of C_2H_2 inside the five atom ring, leading to a new seven atom ring. This species, the cycloheptatrienyl radical, has several peculiar properties very similar to those of cC_5H_5, with particular reference to its stability. This allows this reaction pathway to be fast enough to justify the experimental value of the rate of formation of C_7H_7. This is a new and interesting finding, since undetermined C_7H_7 species in combustion environments are usually ascribed to benzyl radical.

However, it has been shown that the direct formation of benzyl radical from cC_7H_7 is hindered by a large energetic barrier. Interconversion between cycloheptatrienyl and benzyl radicals is possible but requires the formation of cycloheptatriene and toluene, slowing this pathway significantly.

To our knowledge, no dedicated experiments devoted to the identification of cycloheptatrienyl radical in a combustion environment have been carried out. These measurements would be very important to provide further support to the reaction pathway proposed in this work, since the light hydrocarbon growth through odd-ring species could provide an interesting new paradigm for explaining PAH and soot formation in combustion processes.

Acknowledgment. This work was financially supported by PRIN-MIUR 2003-2005.

References and Notes

(1) Kiefer, J. H.; Tranter, R. S.; Wang, H.; Wagner, A. F. *Int. J. Chem. Kinet.* **2001**, *33*, 834−845.
(2) Melius, C. F.; Colvin, M. E.; Marinov, N. M.; Pitz, W. J.; Senkan, S. M. *26th Int. Symp. Combust.* **1996**, *2*, 685.
(3) Moskaleva, L. V.; Mebel, A. M.; Lin, M. C. *26th Int. Symp. Combust.* **1996**, *2*, 521.
(4) Tokmakov, I. V.; Moskaleva, L. V.; Lin, M. C. *Int. J. Chem. Kinet.* **2004**, *36*, 139−151.
(5) Murakami, Y.; Saejung, T.; Ohashi, C.; Fujii, N. *Chem. Lett.* **2003**, *32*, 1112−1113.
(6) Moskaleva, L. V.; Lin, M. C. *Proc. Combust. Inst.* **2002**, *29*, 1319−1327.
(7) Zilberg, S.; Haas, Y. *J. Am. Chem. Soc.* **2002**, *124*, 10683−10691.
(8) Roy, K.; Braun-Unkhoff, M.; Frank, P.; Just, T. *Int. J. Chem. Kinet.* **2001**, *33*, 821−833.
(9) Applegate, B. E.; Bezant, A. J.; Miller, T. A. *J. Chem. Phys.* **2001**, *114*, 4869−4882.
(10) Applegate, B. E.; Miller, T. A.; Barckholtz, T. A. *J. Chem. Phys.* **2001**, *114*, 4855−4868.
(11) D'Anna, A.; Violi, A. *Energy Fuels* **2005**, *19*, 79−86.
(12) Skjoth-Rasmussen, M. S.; Glarborg, P.; Ostberg, M.; Johannessen, J. T.; Livbjerg, H.; Jensen, A. D.; Christensen, T. S. *Combust. Flame* **2004**, *136*, 91−128.
(13) Kunioshi, N.; Touda, M.; Fukutani, S. *Combust. Flame* **2002**, *128*, 292−300.
(14) Richter, H.; Howard, J. B. *Prog. Energy Combust. Sci.* **2000**, *26*, 565−608.
(15) Lindstedt, P.; Maurice, L.; Meyer, M. *Faraday Discuss.* **2001**, *119*, 409−432.
(16) Kunzli, N.; Kaiser, R.; Medina, S.; Studnicka, M.; Chanel, O.; Filliger, P.; Herry, M.; Horak, F.; Puybonnieux-Texier, V.; Quenel, P.; Schneider, J.; Seethaler, R.; Vergnaud, J. C.; Sommer, H. *Lancet* **2000**, *356*, 795−801.
(17) Durant, J. L.; Busby, W. F.; Lafleur, A. L.; Penman, B. W.; Crespi, C. L. *Mutat. Res.-Genet. Toxicol.* **1996**, *371*, 123−157.
(18) Siegmann, K.; Siegmann, H. C. Molecular precursor of soot and quantification of the associated health risk. In *Current Problems in Condensed Matter*; Morán-Lopez, J. L, Ed.; Plenum Press: New York, 1998.
(19) Violi, A.; D'Anna, A.; D'Alessio, A. *Chem. Eng. Sci.* **1999**, *54*, 3433−3442.
(20) Knyazev, V. D.; Slagle, I. R. *J. Phys. Chem. B* **2002**, *106*, 10A−11A.
(21) Schwell, M.; Dulieu, F.; Gee, C.; Jochims, H. W.; Chotin, J. L.; Baumgartel, H.; Leach, S. *Chem. Phys.* **2000**, *260*, 261−279.
(22) Jarzecki, A. A.; Gajewski, J.; Davidson, E. R. *J. Am. Chem. Soc.* **1999**, *121*, 6928−6935.
(23) Wu, T.; Werner, H.; Manthe, U. *Science* **2004**, *306*, 2227−2229.
(24) Dean, A. M. *J. Phys. Chem.* **1985**, *89*, 4600.
(25) Cavallotti, C.; Rota, R.; Carra, S. *J. Phys. Chem. A* **2002**, *106*, 7769−7778.
(26) Cavallotti, C.; Fascella, S.; Rota, R.; Carra, S. *Combust. Sci. Technol.* **2004**, *176*, 705−720.
(27) Fascella, S.; Cavallotti, C.; Rota, R.; Carra, S. *J. Phys. Chem. A* **2004**, *108*, 3829−3843.
(28) Troe, J. *J. Chem. Phys.* **1977**, *66*, 4745.
(29) Frisch, M. J.; Trucks, G. W.; Schlegel, H. B.; Scuseria, G. E.; Robb, M. A.; Cheeseman, J. R.; Zakrzewski, V. G.; Montgomery, J. A., Jr.; Stratmann, R. E.; Burant, J. C.; Dapprich, S.; Millam, J. M.; Daniels, A. D.; Kudin, K. N.; Strain, M. C.; Farkas, O.; Tomasi, J.; Barone, V.; Cossi, M.; Cammi, R.; Mennucci, B.; Pomelli, C.; Adamo, C.; Clifford, S.; Ochterski, J.; Petersson, G. A.; Ayala, P. Y.; Cui, Q.; Morokuma, K.; Malick, D. K.; Rabuck, A. D.; Raghavachari, K.; Foresman, J. B.; Cioslowski, J.;

Ortiz, J. V.; Stefanov, B. B.; Liu, G.; Liashenko, A.; Piskorz, P.; Komaromi, I.; Gomperts, R.; Martin, R. L.; Fox, D. J.; Keith, T.; Al-Laham, M. A.; Peng, C. Y.; Nanayakkara, A.; Gonzalez, C.; Challacombe, M.; Gill, P. M. W.; Johnson, B. G.; Chen, W.; Wong, M. W.; Andres, J. L.; Head-Gordon, M.; Replogle, E. S.; Pople, J. A. *Gaussian 98*, A.7; Gaussian, Inc.: Pittsburgh, PA, 1998.

(30) Becke, A. D. *J. Chem. Phys.* **1993**, *98*, 5648−5652.

(31) Lee, C.; Yang, W.; Parr, R. G. *Phys. Rev. B* **1988**, *37*, 785.

(32) Curtiss, L. A.; Raghavachari, K.; Pople, J. A. *J. Chem. Phys.* **1995**, *103*, 4192−4200.

(33) Truhlar, D. G.; Garrett, B. C.; Klippenstein, S. J. *J. Phys. Chem.* **1996**, *100*, 12771−12800.

(34) Hirschfelder, J. O.; Wigner, E. *J. Chem. Phys.* **1939**, *7*, 616.

(35) Frenklach, M.; Warnatz, J. *Combust. Sci. Technol.* **1987**, *51*, 265.

(36) Vereecken, L.; Peeters, J.; Bettinger, H. F.; Kaiser, R. I.; Schleyer, P. V.; Schaefer, H. F. *J. Am. Chem. Soc.* **2002**, *124*, 2781−2789.